

PAPER NO. 79-2577

VERIFICATION OF SCS DAM-BREACH ROUTING PROCEDURE

by

Fred D. Theurer
Civil Engineer

Design Unit, National Engineering Staff
Engineering Division, Soil Conservation Service
Lanham, Maryland

and

George H. Comer
Hydraulic Engineer

Hydrology Unit, National Engineering Staff
Engineering Division, Soil Conservation Service
Lanham, Maryland

For presentation at the 1979 Winter Meeting
AMERICAN SOCIETY OF AGRICULTURAL ENGINEERS

Hyatt Regency Hotel
New Orleans, LA
December 11-14, 1979

SUMMARY: This paper verifies the SCS dam-breach routing models found in its Technical Release Number 66 (TR-66). This is done by comparing computed results of the TR-66 math models with the measured results of the Waterways Experiment Station (WES) physical models. The comparison shows that the SCS dam-breach procedure is an accurate, well-behaved, easy-to-use procedure for evaluating downstream effects of a simulated dam-breach.



American Society of Agricultural Engineers

St. Joseph, Michigan 49085

Papers presented before ASAE meetings are considered to be the property of the Society. In general, the Society reserves the right of first publication of such papers, in complete form. However, it has no objection to publication, in condensed form, with credit to the Society and the author. Permission to publish a paper in full may be requested from ASAE, P.O. Box 410, St. Joseph, Michigan 49085.

The Society is not responsible for statements or opinions advanced in papers or discussions at its meetings. Papers have not been subjected to the review process by ASAE editorial committees; therefore, are not to be considered as refereed.

VERIFICATION OF SCS DAM-BREACH ROUTING PROCEDURE

Table of Contents

Nomenclature

	<u>Page</u>
Introduction	1
Purpose	1
Technical Release Number 66	1
Waterways Experiment Station Data	2
Breach Hydrograph	3
Peak Discharge and Volume	3
Hydrograph Shape	3
Statistical Verification	5
Valley Hydraulics	10
Calibration of "n-value"	10
Storage-Discharge Relations	10
Breach-Reach Routing	12
Nondimensional Basis	12
TR-66 Math Models	12
Statistical Verification	18
Summary and Conclusions	21
Scope and Applicability	21
Additional Study Needed	21

Nomenclature

A, A^*	\equiv flow area
A_0, A_0^*	\equiv maximum flow area at the downstream section
H_b	\equiv difference between the water surface before the breach and the invert of the breach at the dam
H_0	\equiv maximum stage of water at the dam before breach
I_f	\equiv indicator function; $I_f = 1$ if true and $I_f = 0$ if false
K^*	\equiv linear reservoir storage routing coefficient
k^*	\equiv channel position routing coefficient
k, k_0	\equiv power curve coefficients
L	\equiv distance between breach and downstream section
m	\equiv power curve exponent
n	\equiv Manning's retardance coefficient
N	\equiv number of statistical data points
Q, Q^*	\equiv discharge
Q_i	\equiv discharge of breach hydrograph at time t_i
Q_I	\equiv peak discharge of breach hydrograph
Q_0, Q_0^*	\equiv peak discharge at the downstream section
r, r_m	\equiv correlation coefficients
S, S^*	\equiv valley storage between breach and downstream section
S_0, S_0^*	\equiv maximum valley storage between breach and the downstream section
S_d	\equiv standard deviation
S_e	\equiv standard error of estimate
t, t^*	\equiv time
t_0, t_0^*	\equiv time to peak discharge at the downstream section
V_I	\equiv area under breach hydrograph, volume of flow through breach
W_b	\equiv width of breach
W_d	\equiv width of valley
y, Y, z, Z	\equiv dummy parameters
ϵ	\equiv error term
$\bar{\epsilon}$	\equiv mean error

Note: Terms with an asterisk are nondimensional

INTRODUCTION

Purpose

This paper verifies the math models used by the Soil Conservation Service (SCS) in its "Simplified Dam-breach Routing Procedure," TR-66(1). Solutions of these math models are compared to actual physical model prototype data taken from reports (2, 3) published by the Waterways Experiment Station (WES).

The physio-mathematical basis of the TR-66 math models and the physio-experimental basis of the WES physical models are discussed prior to the numeric comparisons.

The dam-breach procedure is divided into three well-defined components for ease of understanding. Then nondimensional transformations are made to permit generalization of interpretations. And, finally, statistical comparisons are shown to verify the individual components.

Technical Release Number 66

TR-66 has three basic conceptual components: (1) the breach hydrograph, (2) the valley hydraulics, and (3) the breach-reach routing. The usual math models for these components have been simplified to make the solution more tractable while retaining the essential characteristics necessary to evaluate downstream effects of a simulated dam-breach. Before TR-66 was available, math models for the first and third components were sophisticated and required difficult numeric solutions, but in TR-66 they have been converted to simple, almost effortless, solutions.

The breach hydrograph has been reduced to an analytic expression requiring only a determination of: (1) the instantaneous peak discharge through the breach (Q_T), (2) the total volume of flow through the breach (V_T), and (3) choice of shape based on the immediate downstream valley hydraulic characteristics.

The valley hydraulics determination requires only standard state-of-the-art rating curve calculations; i.e., some form of steady-state water surface profile computations. These computations can be based on current methods assuming uniform, constant-discharge non-uniform, or spatially-varied steady flow to approximate the actual instantaneous unsteady flow water surface profile at the time to peak discharge of the downstream point of interest. The resulting rating curve is converted into a storage-discharge power curve of the form $Q = k S^m$. Of course, the accuracy of the resulting storage-discharge relation depends on the method used.

The breach-reach routing model was derived from a simultaneous storage and kinematic routing model called the Att-Kin (Attenuation-Kinematic) model. A dry-bed assumption is made. This dry-bed assumption, the instantaneous breach assumption, the single-valued storage-discharge relation, analytic breach hydrograph, and certain numeric approximations lead to a closed-form solution of the dam-breach problem. Furthermore, the mathematically exact nondimensional basis was found that permitted a presolution so that the user need only to read a chart (ES-212 of TR-66) to determine the resulting downstream peak discharge when given the breach hydrograph data (peak, volume, and shape) and the single-valued storage-discharge parameters (k and m).

Waterways Experiment Station Data

The WES data are based upon two series of laboratory flume experiments performed in the early 1960's. The primary purposes of the experiments were to verify the Schoklitsch instantaneous breach peak discharge formula (which they did) and to study the behavior of the negative flood wave upstream of the breach. Secondary interests were the entire breach hydrograph and the behavior of the positive flood wave downstream of the breach. Since the downstream data were of secondary interest, they were not as detailed or rigorously collected and processed. Therefore, the downstream data that were published contain significant experimental error. For example, they indicate that during a few of the test runs, peak discharge increased as the flood wave moved downstream. Also, some test run data imply that, at times, more water was in the downstream flume than passed through the breach. There is no physical explanation for these phenomena; therefore, there had to be some error in the data as measured or as processed. However, it is believed that these errors are not so great as to invalidate the data; some differences between the TR-66 math model predictions and WES prototype data are due to experimental error rather than to inaccuracy of the math models.

The WES prototype model was a wooden rectangular flume, 4 feet wide by 400 feet long set on a 0.005 slope. A removable gate that could be changed for various heights and widths was placed at the midpoint (200 feet). Water was let in behind the gate until it reached a 1-foot stage at the gate. The gate was then instantaneously removed and subsequent data collected.

Data were collected upstream of the gate and processed to determine the discharge hydrograph at the breach (breach hydrograph). Data for downstream stage-discharge hydrographs were collected at stations located 25, 80, and 150 feet downstream of the gate. The downstream data consisted of point gage readings for stage and surface velocity estimates for determining the instantaneous average velocity at each station. Surface velocity was obtained by timing the movement of confetti as it passed beneath a plexiglass grid. Surface velocity was converted to average velocity by calibration of steady-state conditions. Obviously, the stage and velocity determination are rich sources of experimental error.

Two series of runs were made. The first series was with an unmodified or "smooth condition" flume; i.e., the flume had hydraulically smooth boundaries. The second series was with a modified or "rough condition" flume; i.e., the flume had $3/4" \times 3/4" \times 1/4"$ angles spaced 6 inches apart transverse to the flow.

Twelve dry-bed runs were made for the smooth series and eight for the rough. No base flow was added before or during any of these twenty runs.

The smooth condition runs are identified as Run 1.1, 1.2, ..., 12.1. The rough condition runs are identified as Run 1.2, 2.2, ..., 12.2.

The volume of flow through the breach was determined by computing the total volume behind the gate before the breach (always 400 ft^3) less any dead volume caught below the gate invert and behind angles upstream of the gate.

BREACH HYDROGRAPH

Peak and Volume Determination

The analytic hydrograph peak used in verifying the TR-66 dam-breach procedure was determined by the Schoklitsch equation. This equation was derived from the one-dimensional unsteady flow equations assuming an instantaneous full-depth full-width breach. Schoklitsch empirically modified the equation using coefficients to correct for partial-width and partial-depth openings. The conclusion of the WES studies was that a modified combined partial-width partial-depth coefficient is valid for predicting the instantaneous hydrograph peak at the breach. This modified Schoklitsch equation is

$$Q_I = \left(\frac{8}{27}\right) W_b \left(\frac{W_d}{W_b} \frac{H_o}{H_b}\right)^{0.28} \sqrt{g} H_b^{3/2} \dots \quad \text{Eq. 1}$$

where

Q_I \equiv maximum or peak discharge at the breach

W_b \equiv width of the breach

W_d \equiv width of the dam

H_o \equiv depth of water at the dam

H_b \equiv depth of the breach

g \equiv acceleration of gravity.

The peaks of the analytic breach hydrographs determined by Eq. 1 are almost all conservative compared to the WES data; i.e., measured peaks are higher than the predicted peaks in only two cases. These data are shown in Table No. 1, Breach Hydrograph Data. Also shown are the associated volumes of flow through the breach.

The greatest differences between measured and calculated peaks are associated with runs 8 and 12. These two runs were made with partial-depth breaches and should have been unaffected by downstream conditions. The greatest discrepancy is associated with run 12.1. There is no explanation why the measured peak on this run should be less than the peak of run 12.2. We attribute this to experimental error in the determination of the peak.

The volume of the analytic breach hydrograph is simply the drainable volume in the reservoir.

Hydrograph Shape

The requirements for the analytic breach hydrograph were: (a) it must start with the Schoklitsch peak, (b) it must conserve mass, (c) it must decrease monotonically, (d) it must be mathematically easy to use, and (e) it must fit the data. The general shape of the measured hydrographs led to the selection of two shapes to be used. For the first set of runs on a smooth channel, a triangular shape was selected. A curvilinear shape (exponential) was selected for the runs on the rough channel.

TABLE NO. 1
BREACH HYDROGRAPH DATA

Run No.	Smooth Condition		Rough Condition		Schoklitsch Breach Peak Discharge (Q_I) cfs
	Measured Peak Discharge (Q_{max}) cfs	Volume Breach Hydrograph (V_I) ft ³	Measured Peak Discharge (Q_{max}) cfs	Volume Breach Hydrograph (V_I) ft ³	
1	6.50	400	6.41	350	6.72
2	4.54	400	4.11	350	4.57
3	2.67	400	2.47	350	2.72
4	1.70	400	1.54	350	1.62
5	1.16	400	--	--	1.20
6	0.77	400	--	--	0.81
7	3.57	336	3.42	306	3.70
8	1.42	204	1.43	189	1.66
9	0.67	111	--	--	0.73
10	0.43	76	--	--	0.46
11	2.52	336	2.53	306	2.52
12	0.56	204	0.63	189	0.67

Note: Runs 5, 6, 9, and 10 for the rough channel condition were not done.

The triangular hydrograph is defined by

$$Q_i = Q_I [1 - (t^*/2)] I_f [t^* < 2] \quad \text{Eq. 2}$$

The curvilinear hydrograph is defined by

$$Q_i = Q_I e^{-t^*} \quad \text{Eq. 3}$$

and, the normalized discharge is defined by:

$$Q_i^* = Q_i / Q_I \quad \text{Eq. 4}$$

where

- Q_i = the discharge at time t^*
 Q_I = the breach peak determined by the Schoklitsch equation
 t^* = $t \left(\frac{Q_I}{V_I} \right)$
 t = time
 V_I = volume of the breach hydrograph
 $I_f [t^* \leq 2]$ = indicator function; $I_f = 1$ if $t^* \leq 2$, $I_f = 0$ if $t^* > 2$

These hydrograph equations were used to generate the breach hydrograph. Q_I was determined by the Schoklitsch equation and V_I was the drainable volume in the reservoir. The discharge is normalized by Q_I and all analyses are made on the normalized data.

Statistical Verification

Statistical measures for adherence of the TR-66 analytic breach hydrograph to the measured WES data are difficult because both the hydrograph shape and peak are involved. In addition, indices of goodness to fit for time series traces are not universally accepted. There are also properties of the hydrographs that tend to enhance the meaning of some statistical measures; e.g. the volumes of both the analytic and measured hydrographs are the same and both decrease monotonically, therefore some minimum correlation is guaranteed.

The first source of variation between the analytic and measured hydrographs are the differences in the peaks. The peaks determined by the Schoklitsch equation are lower than the measured peaks in only two cases. If all the analytic hydrographs started at the measured peaks, the fits would have been better for some hydrographs but not for all.

The peaks determined by the Schoklitsch equation resulted in a better prediction of the downstream peaks. This indicated that there is less error in the Schoklitsch calculation than in the experimental determination of the peaks.

The second source of variation is the shape itself. The two shapes selected met all our criteria for the analytic shape. Figure 1, Breach Hydrograph - Smooth Channel and Figure 2, Breach Hydrograph - Rough Channel, show the analytic hydrographs and the measured points for the smooth and rough channels.

The error parameters calculated were

1. Mean error

$$\bar{\epsilon} = \int_0^T \epsilon_i dt \quad \text{Eq. 5}$$

where

$$\epsilon_i = (Q_{ci}^* - Q_{mi}^*)$$

Q_{ci}^* \equiv normalized computed discharge from the analytic breach hydrograph

Q_{mi}^* \equiv normalized measured discharge from the WES data

T \equiv 2.0 for the triangular hydrographs (smooth conditions)
and ∞ for the curvilinear hydrographs (rough conditions)

2. Average absolute error

$$\overline{|\epsilon|} = \int_0^T |\epsilon_i| dt \quad \text{Eq. 6}$$

3. $\epsilon_{\max} = \text{Max}(\epsilon) \equiv$ maximum overestimation error

4. $\epsilon_{\min} = \text{Min}(\epsilon) \equiv$ maximum underestimation error.

These statistical measures were computed for each hydrograph. For the smooth channel (triangular) hydrographs, the values were computed up to a t^* of 2 to give the entire volume of the breach in the analytic hydrograph. The $\bar{\epsilon}$ is the volume remaining under the measured hydrograph that is yet to pass the breach when the analytic hydrograph is zero.

The curvilinear hydrographs were computed to a t^* of ∞ . The WES data covered times up to a t^* of about 2.4. Beyond this time, the measured data were extrapolated by an exponential decay from the last measured time so the remaining volume in the reservoir was emptied at $t^* = \infty$. The calculations beyond a t^* of 2.4 were done analytically by integrals and the sums added to the sums of the discrete points for computing the statistics. The $\bar{\epsilon}$ for these cases is zero since mass is conserved.

The correlation coefficients and modified correlation coefficients were also calculated. McCuen and Snyder (6) point out that the Pearson product-moment correlation coefficient for a hydrograph can be quite high even when the fit is not good because it does not account for differences in volumes. They proposed a modified correlation coefficient which was used here. The modified correlation coefficient is computed as

$$r_m = \frac{\sum zy}{\sum z^2} \quad \text{Eq. 7}$$

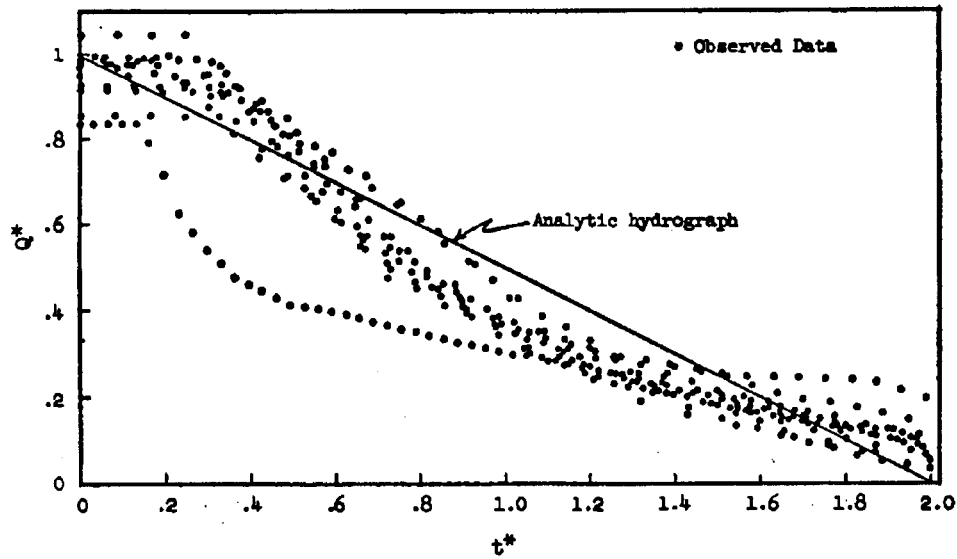


Figure 1. Breach Hydrograph - Smooth Channel

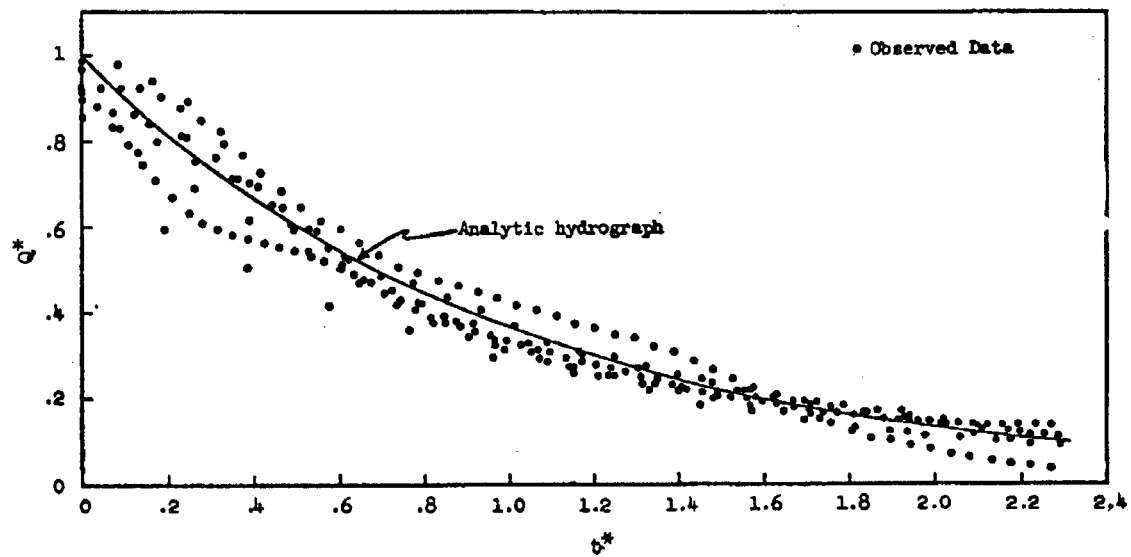


Figure 2. Breach Hydrograph - Rough Channel

where

$$\Sigma zy = \Sigma [(Z - \bar{Z})(Y - \bar{Y})]$$

$$\Sigma z^2 = \Sigma (Z - \bar{Z})^2$$

Y and Z = ordinates of the measured and analytic hydrographs.

The larger of the two hydrographs is used as the Z ordinates.

Table 2, Statistical Data - Breach Hydrograph, gives all the statistical parameters calculated. Most of the TR-66 analytic hydrographs are excellent fits. The largest errors are overestimates, which means the analytic hydrographs are conservative. The average mean error for all hydrographs combined is just under 5 percent with a mean absolute error of 1.48 percent. The triangular hydrograph does not fit the smooth data as well as the curvilinear hydrograph fits the rough channel data. However, the smooth channel data fit is very good with the exception of run 12.1.

The correlation coefficients were all very high which was expected. Even the modified correlation coefficients were consistently above 0.8 with one exception in each set of runs. The average correlation coefficients for all the hydrographs were 0.965 and 0.991 for the smooth and rough condition channels respectively.

Based on these statistics, the triangular shape is a reasonable representation of the breach hydrograph for the smooth channel data and the curvilinear shape is a good representation of the breach hydrograph for the rough channel data. These analytic hydrographs and the Schoklitsch equation for the peaks were used in developing and verifying the TR-66 routing procedure.

TABLE NO. 2
STATISTICAL DATA - BREACH HYDROGRAPH

Run No.	$\bar{\epsilon}$	$ \bar{\epsilon} $	r	r_m	ϵ at $t^*=0$	ϵ_{max}	ϵ_{min}
<u>Smooth Condition</u>							
1.1	.038	.121	.986	.862	.033	.119	.076
2.1	.014	.103	.991	.879	.007	.085	.099
3.1	.050	.154	.963	.869	.018	.148	.135
4.1	.033	.163	.965	.850	-.049	.144	.171
5.1	.075	.126	.977	.973	.033	.133	.073
6.1	.070	.144	.963	.906	.049	.149	.120
7.1	.086	.164	.973	.868	.035	.167	.098
8.1	.109	.156	.968	.959	.145	.170	.085
9.1	.102	.168	.959	.953	.082	.164	.096
10.1	.007	.186	.936	.867	.065	.144	.194
11.1	.084	.156	.971	.875	.000	.158	.105
12.1	.311	.334	.928	.661	.164	.342	.075
MEAN	.082	.164	.965	.877	.049	.342	.194
<u>Rough Condition</u>							
1.2	0	.245	.966	.796	.046	.230	.028
2.2	0	.106	.999	.862	.101	.103	.012
3.2	0	.074	.997	.946	.092	.099	.028
4.2	0	.129	.987	.893	.049	.074	.110
7.2	0	.116	.996	.993	.076	.081	.026
8.2	0	.096	.997	.920	.139	.145	.012
11.2	0	.108	.994	.894	-.004	.062	.112
12.2	0	.120	.993	.833	.060	.146	.035
MEAN	0	.124	.991	.892	.070	.230	.112
COMBINED CONDITIONS	.049	.148	.975	.883	.057	.342	.194

VALLEY HYDRAULICS

Calibration of "n-value"

The WES data contain steady-state n-value calibrations of the entire flow range for each channel condition. The smooth channel condition had a near constant n-value. It was: $n \approx 0.009$. The rough channel had an n-value that ranged systematically from 0.035 to 0.150. The higher n-value was at the lower discharges.

Storage-Discharge Relations

Water surface profiles were calculated by the authors assuming constant discharge non-uniform steady flow for each channel condition. The calibrated n-values were used. It was found that the flow was supercritical for the smooth channel and subcritical for the rough. Furthermore, the flows were very nearly uniform at the downstream data stations for each channel condition. Consequently, uniform steady flow was assumed to be applicable for each channel condition. The resulting power curve for each channel condition gave an excellent curve fit over the entire flow range. The power curve represents the flow area-discharge relation, which can be converted directly to a storage-discharge relation.

The flow area-discharge power curve is: $Q = k_0 A^m$, but $S = LA$; Eq. 8
therefore, the storage-discharge power curve is

$$Q = k S^m, \text{ where } k = k_0/L^m \quad \text{Eq. 9}$$

Table No. 3, Flow Area-Discharge Parameters, lists the power curve parameters for each channel condition. Figure No. 3, Valley Hydraulics, Rating Curves, compares the actual rating curves to the power curve fit for each channel condition.

TABLE NO. 3
FLOW AREA-DISCHARGE PARAMETERS

Channel Condition	Parameters	
	k_0	m
smooth	4.633	5/3
rough	0.600	2

$$Q = k_0 A^m$$

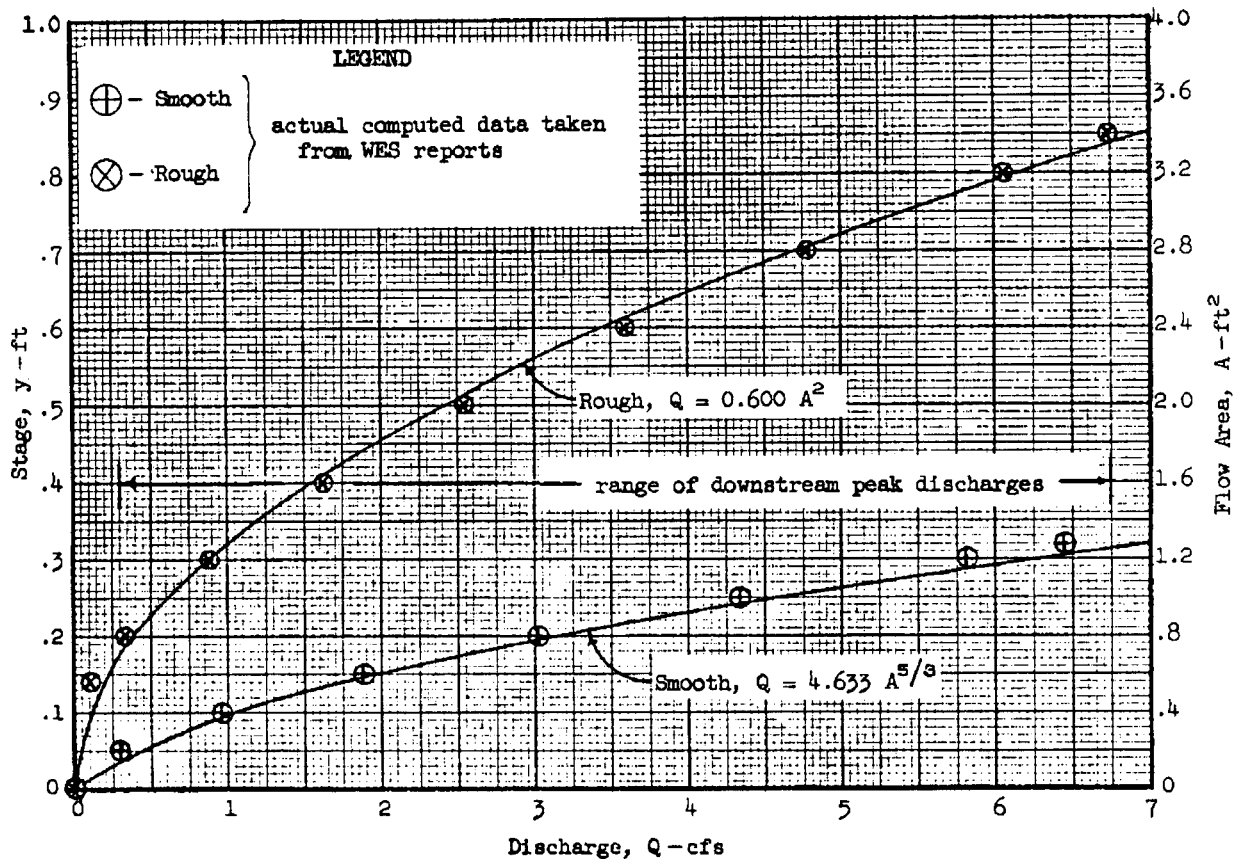


Figure 3. Valley Hydraulics, Rating Curve

BREACH-REACH ROUTING

Nondimensional Basis

In TR-66, a mathematically exact nondimensional basis is used to relate the breach hydrograph to the valley hydraulics. This basis allows two different situations with similar geometric, hydraulic, and hydrologic characteristics to have identical nondimensional responses. The nondimensional relationships are:

1. all discharges, $Q^* = Q/Q_I$ Eq. 10

2. all times, $t^* = t(Q_I/V_I)$ Eq. 11

3. all flow areas, $A^* = A/[(Q_I/k_o)^{(1/m)}]$ Eq. 12

4. all storages or volumes, $S^* = S/V_I$ Eq. 13

All nondimensional relationships lead to the following channel position routing coefficient:

$$k^* = (Q_I/k_o)(L/V_I)^m \quad \text{Eq. 14}$$

Therefore, different valley systems that have the same power curve exponent m and the same shape breach hydrographs will have identical nondimensional responses at the same k^* , i.e., Q_0^* , t_0^* , A_0^* and S_0^* will be exactly the same for each system at the corresponding k^* channel positions.

TR-66 Math Models

The triangular shape breach hydrograph was appropriate for the smooth channel conditions; the curvilinear shape was appropriate for the rough.

The breach-reach routing math models used in TR-66 are:

1. For the triangular breach hydrograph,

$$t_0^* = m(1+Q_0^*)[Q_0^{*(-1/m)} - 1] \quad \text{Eq. 15}$$

$$k^* = \{V^* - [Q_0^{*2}(1-Q_0^*)]\}^m / Q_0^* \quad \text{Eq. 16}$$

$$V^* = \{t_0^*[1 - (t_0^*/4)]I_f[t_0^* \leq 2]\} + \{I_f[t_0^* > 2]\} \quad \text{Eq. 17}$$

2. For the curvilinear breach hydrograph,

$$t_0^* = m[Q_0^{*(-1/m)} - 1] \quad \text{Eq. 18}$$

$$k^* = \{[1 - e^{-t_0^*}] + [(Q_0^{*2}/2) \ln Q_0^*]\}^m / Q_0^* \quad \text{Eq. 19}$$

Equations 15 through 17 or 18 and 19 are to be solved simultaneously.

The appropriate routing formulas in TR-66 were solved at the downstream WES data stations. Table No. 4, Breach-Reach Routing - Smooth Channel, and Table No. 5, Breach-Reach Routing - Rough Channel, summarize the pertinent results.

TABLE NO. 4
BREACH-REACH ROUTING - SMOOTH CHANNEL

Test No.	Method	L, ft	Q ₀ , cfs	t ₀ , sec	A ₀ , ft ²	k*	Q ₀ *	t ₀ *	A ₀ *	S ₀ *
1.1	WES	0	6.72	0	--	0	1	0	--	0
	TR-66	0	6.72	0	1.25	0	1	0	1	0
	WES	25	5.6	15	1.28	0.014	0.833	0.252	1.024	0.080
	TR-66	25	6.26	5	1.20	0.014	0.932	0.079	0.959	0.075
	WES	80	4.7	31	1.04	0.099	0.699	0.521	0.832	0.208
	TR-66	80	5.53	15	1.11	0.099	0.822	0.260	0.889	0.222
	WES	150	4.1	37	1.00	0.283	0.610	0.622	0.800	0.375
	TR-66	150	4.83	30	1.03	0.283	0.718	0.499	0.820	0.384
2.1	WES	0	4.57	0	--	0	1	0	--	0
	TR-66	0	4.57	0	0.99	0	1	0	1	0
	WES	25	4.1	25	0.96	0.010	0.897	0.286	0.968	0.060
	TR-66	25	4.32	5	0.96	0.010	0.945	0.063	0.966	0.060
	WES	80	4.0	32	0.96	0.068	0.875	0.366	0.968	0.192
	TR-66	80	3.89	18	0.90	0.068	0.852	0.205	0.908	0.180
	WES	150	4.0	45	1.00	0.192	0.875	0.514	1.008	0.375
	TR-66	150	3.48	34	0.84	0.192	0.761	0.392	0.849	0.316
3.1	WES	0	2.72	0	--	0	1	0	--	0
	TR-66	0	2.72	0	0.73	0	1	0	1	0
	WES	25	2.6	47	0.64	0.006	0.956	0.320	0.881	0.040
	TR-66	25	2.61	7	0.71	0.006	0.958	0.046	0.975	0.044
	WES	80	2.6	41	0.72	0.040	0.956	0.279	0.991	0.144
	TR-66	80	2.41	22	0.67	0.040	0.885	0.149	0.929	0.135
	WES	150	2.5	55	0.72	0.114	0.919	0.374	0.991	0.270
	TR-66	150	2.20	42	0.64	0.114	0.810	0.284	0.881	0.240
4.1	WES	0	1.62	0	--	0	1	0	--	0
	TR-66	0	1.62	0	0.53	0	1	0	1	0
	WES	25	1.7	17	0.56	0.003	1.049	0.069	1.052	0.035
	TR-66	25	1.57	8	0.52	0.003	0.969	0.033	0.981	0.033
	WES	80	1.4	60	0.56	0.024	0.864	0.243	1.052	0.112
	TR-66	80	1.48	27	0.50	0.024	0.911	0.108	0.946	0.101
	WES	150	1.3	70	0.52	0.068	0.802	0.284	0.977	0.195
	TR-66	150	1.38	51	0.48	0.068	0.851	0.206	0.908	0.181

TABLE NO. 4 (Cont'd.)
BREACH-REACH ROUTING - SMOOTH CHANNEL

Test No.	Method	L, ft	Q ₀ , cfs	t ₀ , sec	A ₀ , ft ²	k*	Q* ₀	t* ₀	A* ₀	S* ₀
5.1	WES	0	1.20	0	--	0	1	0	--	0
	TR-66	0	1.20	0	0.44	0	1	0	1	0
	WES	25	1.20	30	0.44	0.003	1	0.090	0.990	0.028
	TR-66	25	1.17	9	0.44	0.003	0.974	0.028	0.984	0.027
5.1	WES	80	0.95	40	0.44	0.018	0.792	0.120	0.990	0.088
	TR-66	80	1.11	30	0.42	0.018	0.924	0.090	0.954	0.085
	WES	150	0.90	80	0.40	0.051	0.750	0.240	0.900	0.150
	TR-66	150	1.05	57	0.41	0.051	0.871	0.171	0.920	0.153
6.1	WES	0	0.81	0	--	0	1	0	--	0
	TR-66	0	0.81	0	0.35	0	1	0	1	0
	WES	25	0.65	30	0.36	0.002	0.802	0.061	1.025	0.023
	TR-66	25	0.79	11	0.35	0.002	0.979	0.022	0.987	0.022
6.1	WES	80	0.70	60	0.36	0.012	0.864	0.122	1.025	0.072
	TR-66	80	0.76	35	0.34	0.012	0.938	0.071	0.962	0.068
	WES	150	0.70	95	0.36	0.034	0.864	0.192	1.025	0.135
	TR-66	150	0.72	66	0.33	0.034	0.894	0.135	0.935	0.123
7.1	WES	0	3.70	0	--	0	1	0	--	0
	TR-66	0	3.70	0	0.87	0	1	0	1	0
	WES	25	3.55	22	0.80	0.011	0.959	0.242	0.916	0.060
	TR-66	25	3.49	6	0.84	0.011	0.942	0.066	0.965	0.063
7.1	WES	80	3.30	27	0.80	0.073	0.892	0.297	0.916	0.190
	TR-66	80	3.13	20	0.79	0.073	0.846	0.215	0.905	0.188
	WES	150	3.20	42	0.84	0.208	0.865	0.463	0.961	0.375
	TR-66	150	2.79	37	0.74	0.208	0.753	0.412	0.843	0.329
8.1	WES	0	1.66	0	--	0	1	0	--	0
	TR-66	0	1.66	0	0.54	0	1	0	1	0
	WES	25	1.50	18	0.48	0.011	0.904	0.146	0.889	0.059
	TR-66	25	1.56	8	0.52	0.011	0.941	0.067	0.964	0.064
8.1	WES	80	1.30	55	0.48	0.075	0.783	0.448	0.889	0.188
	TR-66	80	1.40	27	0.49	0.075	0.844	0.219	0.903	0.191
	WES	150	1.20	72	0.48	0.215	0.723	0.586	0.889	0.353
	TR-66	150	1.24	52	0.45	0.215	0.750	0.420	0.841	0.334

TABLE NO. 4 (Cont'd.)
BREACH-REACH ROUTING - SMOOTH CHANNEL

Test No.	Method	L, ft	Q ₀ , cfs	t ₀ , sec	A ₀ , ft ²	k*	Q ₀ *	t ₀ *	A ₀ *	S ₀ *
9.1	WES	0	0.73	0	--	0	1	0	--	0
	TR-66	0	0.73	0	0.33	0	1	0	1	0
	WES	25	0.60	19	0.32	0.013	0.822	0.125	0.970	0.072
	TR-66	25	0.68	11	0.32	0.013	0.935	0.075	0.961	0.071
	WES	80	0.60	52	0.32	0.091	0.822	0.342	0.970	0.231
	TR-66	80	0.61	38	0.29	0.091	0.829	0.247	0.894	0.213
	WES	150	0.55	90	0.32	0.260	0.753	0.592	0.970	0.432
	TR-66	150	0.53	72	0.27	0.260	0.728	0.474	0.827	0.369
10.1	WES	0	0.46	0	--	0	1	0	--	0
	TR-66	0	0.46	0	0.25	0	1	0	1	0
	WES	25	0.42	33	0.20	0.016	0.913	0.200	0.800	0.066
	TR-66	25	0.43	14	0.24	0.016	0.929	0.083	0.957	0.079
	WES	80	0.35	60	0.20	0.108	0.761	0.363	0.800	0.211
	TR-66	80	0.37	45	0.22	0.108	0.815	0.274	0.885	0.233
	WES	150	0.35	110	0.20	0.308	0.716	0.666	0.800	0.395
	TR-66	150	0.33	87	0.20	0.308	0.708	0.527	0.813	0.401
11.1	WES	0	2.52	0	--	0	1	0	--	0
	TR-66	0	2.52	0	0.69	0	1	0	1	0
	WES	25	3.00	20	0.64	0.007	1.190	0.150	0.922	0.048
	TR-66	25	2.40	7	0.67	0.007	0.953	0.052	0.972	0.050
	WES	80	2.3	40	0.64	0.050	0.913	0.300	0.922	0.152
	TR-66	80	2.2	23	0.64	0.050	0.872	0.170	0.921	0.152
	WES	150	2.05	60	0.64	0.142	0.813	0.450	0.922	0.286
	TR-66	150	1.99	43	0.60	0.142	0.791	0.324	0.869	0.269
12.1	WES	0	0.67	0	--	0	1	0	--	0
	TR-66	0	0.67	0	0.31	0	1	0	1	0
	WES	25	0.60	30	0.28	0.004	0.896	0.099	0.893	0.034
	TR-66	25	0.65	12	0.31	0.004	0.964	0.039	0.978	0.038
	WES	80	0.52	50	0.32	0.030	0.776	0.164	1.021	0.125
	TR-66	80	0.60	38	0.29	0.030	0.900	0.125	0.939	0.115
	WES	150	0.42	90	0.24	0.087	0.627	0.296	0.766	0.176
	TR-66	150	0.56	73	0.28	0.087	0.833	0.239	0.896	0.207

TABLE NO. 5
BREACH-REACH ROUTING - ROUGH CHANNEL

Test No.	Method	L, ft	Q ₀ , cfs	t ₀ , sec	A ₀ , ft ²	k*	Q ₀ *	t ₀ *	A ₀ *	S ₀ *
1.2	WES	0	6.72	0	--	0	1	0	--	0
	TR-66	0	6.72	0	3.35	0	1	0	1	0
	WES	25	3.4	18	2.00	0.057	0.506	0.346	0.598	0.143
	TR-66	25	4.91	13	2.86	0.057	0.731	0.258	0.855	0.204
	WES	80	2.1	49	1.80	0.585	0.313	0.941	0.538	0.411
	TR-66	80	3.13	47	2.28	0.585	0.466	0.909	0.683	0.522
	WES	150	1.6	99	1.60	2.06	0.238	1.901	0.478	0.686
	TR-66	150	1.94	97	1.80	2.06	0.288	1.813	0.537	0.770
2.2	WES	0	4.57	0	--	0	1	0	--	0
	TR-66	0	4.57	0	2.76	0	1	0	1	0
	WES	25	3.9	17	2.00	0.039	0.853	0.222	0.725	0.143
	TR-66	25	3.49	16	2.41	0.039	0.764	0.210	0.874	0.172
	WES	80	2.2	54	1.84	0.398	0.481	0.705	0.667	0.421
	TR-66	80	2.36	56	1.99	0.398	0.517	0.734	0.719	0.454
	WES	150	1.6	103	1.64	1.40	0.350	1.345	0.594	0.703
	TR-66	150	1.57	114	1.62	1.40	0.344	1.491	0.586	0.693
3.2	WES	0	2.72	0	--	0	1	0	--	0
	TR-66	0	2.72	0	2.13	0	1	0	1	0
	WES	25	2.0	32	1.76	0.023	0.735	0.249	0.827	0.126
	TR-66	25	2.18	21	1.91	0.023	0.803	0.160	0.896	0.136
	WES	80	1.6	62	1.60	0.237	0.588	0.482	0.751	0.366
	TR-66	80	1.58	71	1.62	0.237	0.582	0.552	0.763	0.371
	WES	150	1.3	115	1.44	0.833	0.478	0.894	0.676	0.617
	TR-66	150	1.14	143	1.38	0.833	0.417	1.109	0.646	0.590
4.2	WES	0	1.62	0	--	0	1	0	--	0
	TR-66	0	1.62	0	1.64	0	1	0	1	0
	WES	25	1.3	36	1.52	0.014	0.802	0.167	0.925	0.109
	TR-66	25	1.36	26	1.50	0.014	0.837	0.123	0.915	0.107
	WES	80	1.1	100	1.36	0.141	0.679	0.463	0.828	0.311
	TR-66	80	1.04	90	1.32	0.141	0.641	0.417	0.801	0.301
	WES	150	1.0	160	1.30	0.496	0.617	0.741	0.791	0.557
	TR-66	150	0.79	179	1.15	0.496	0.488	0.829	0.699	0.492

TABLE NO. 5 (Cont'd.)
BREACH-REACH ROUTING - ROUGH CHANNEL

Test No.	Method	L, ft	Q ₀ , cfs	t ₀ , sec	A ₀ , ft ²	k*	Q ₀ *	t ₀ *	A ₀ *	S ₀ *
7.2	WES	0	3.70	0	--	0	1	0	--	0
	TR-66	0	3.70	0	2.48	0	1	0	1	0
	WES	25	2.8	26	1.96	0.041	0.757	0.314	0.789	0.160
	TR-66	25	2.81	18	2.16	0.041	0.759	0.217	0.871	0.177
	WES	80	1.8	60	1.72	0.421	0.486	0.725	0.693	0.450
	TR-66	80	1.89	63	1.77	0.421	0.510	0.758	0.714	0.464
	WES	150	1.4	116	1.52	1.48	0.378	1.403	0.612	0.745
	TR-66	150	1.24	128	1.44	1.48	0.335	1.542	0.579	0.705
8.2	WES	0	1.66	0	--	0	1	0	--	0
	TR-66	0	1.66	0	1.66	0	1	0	1	0
	WES	25	1.1	35	1.32	0.048	0.663	0.307	0.794	0.175
	TR-66	25	1.24	27	1.44	0.048	0.745	0.236	0.863	0.190
	WES	80	0.86	80	1.20	0.496	0.518	0.703	0.721	0.508
	TR-66	80	0.81	94	1.16	0.496	0.488	0.829	0.699	0.492
	WES	150	0.72	155	1.16	1.74	0.434	1.361	0.697	0.921
	TR-66	150	0.52	193	0.93	1.74	0.312	1.694	0.559	0.737
11.2	WES	0	2.52	0	--	0	1	0	--	0
	TR-66	0	2.52	0	2.05	0	1	0	1	0
	WES	25	2.15	30	1.76	0.028	0.853	0.247	0.859	0.144
	TR-66	25	1.99	22	1.82	0.028	0.789	0.177	0.888	0.149
	WES	80	1.55	72	1.56	0.287	0.615	0.593	0.761	0.408
	TR-66	80	1.41	74	1.53	0.287	0.559	0.613	0.747	0.400
	WES	150	1.20	132	1.44	1.01	0.476	1.087	0.703	0.706
	TR-66	150	0.98	150	1.28	1.01	0.390	1.237	0.625	0.628
12.2	WES	0	0.67	0	--	0	1	0	--	0
	TR-66	0	0.67	0	1.06	0	1	0	1	0
	WES	25	0.48	84	0.96	0.020	0.716	0.298	0.908	0.127
	TR-66	25	0.55	41	0.95	0.020	0.815	0.147	0.903	0.126
	WES	80	0.40	140	0.84	0.200	0.597	0.496	0.795	0.356
	TR-66	80	0.40	142	0.82	0.200	0.602	0.504	0.776	0.347
	WES	150	0.40	235	0.84	0.703	0.597	0.833	0.795	0.667
	TR-66	150	0.30	284	0.70	0.703	0.441	1.008	0.664	0.557

The pertinent results for each data station are (1) the peak discharge (Q_0), (2) the time to peak discharge (t_0), (3) the maximum flow area (A_0), and (4) the valley storage (S_0) between the breach and the respective station at the time to peak discharge. The maximum flow area for unsteady flow (and, therefore, in the WES data) does not necessarily occur at the time to peak discharge. However, any math model that uses a single-valued rating curve assumes that these times coincide. The authors selected the actual maximum flow area from the WES data to compare to the predicted maximum flow area from TR-66.

Figures No. 4 and 5 are a plot of Q_0^* versus k^* for the respective WES channel conditions. Ordered data plots are also shown.

The plots also contain some additional information that is useful in interpreting results obtained through TR-66. The figures show bounds that represent physio-mathematical limits of unsteady flow models. The upper limits are derived from kinematic and conservation of mass principles and the lower is derived from storage routing models. These physical laws require that the immediate downstream channel ($k^* = 0$) have the same peak discharge as the breach hydrograph; i.e., $Q_0^* = 1$ at $k^* = 0$. They also require that the peak discharge decrease monotonically to zero as the flood wave moves downstream; i.e., $Q_0^* \rightarrow 0$ as $k^* \rightarrow \infty$ and $dQ_0^*/dk^* < 0$ for all k^* . The TR-66 math models behave according to these laws.

The physio-mathematical bounds completely contain the entire range of k^* . The kinematic model and the conservation of mass determine the upper bound; i.e. $Q_0^* < 1$ for $k^* \leq 1$ and $Q_0^* < 1/k^*$ for $k^* > 1$.

The storage routing model is a lower bound. A linear reservoir assumption ($m = 1$) is a good approximation for the storage routing model as long as the storages are identical for the resulting peak discharge. This lower bound is:

1. For the curvilinear shape breach hydrograph,

$$Q_0^* \geq k^* \left[\frac{k^*}{1-k^*} \right], \text{ where: } K^* = S_0^*/Q_0^* \quad \text{Eq. 20}$$

2. For the triangular hydrograph

$$Q_0^* \geq 1 - \{(k^*/2) \ln[1+(2/k^*)]\} \quad \text{Eq. 21}$$

The corresponding channel position routing coefficient for the linear reservoir assumption is:

$$k^* = (K^* Q_0^*)^m / Q_0^* \quad \text{Eq. 22}$$

Statistical Verification

Table No. 6, Statistical Data - Breach-Reach Routing, summarizes the important statistical measures for each separate channel condition and for both when combined. While it was possible to extract the peak discharge, time to peak discharge, and valley storage immediately downstream ($k^* = 0$) from the WES data, it was not possible to determine the flow area because the breach invert was not

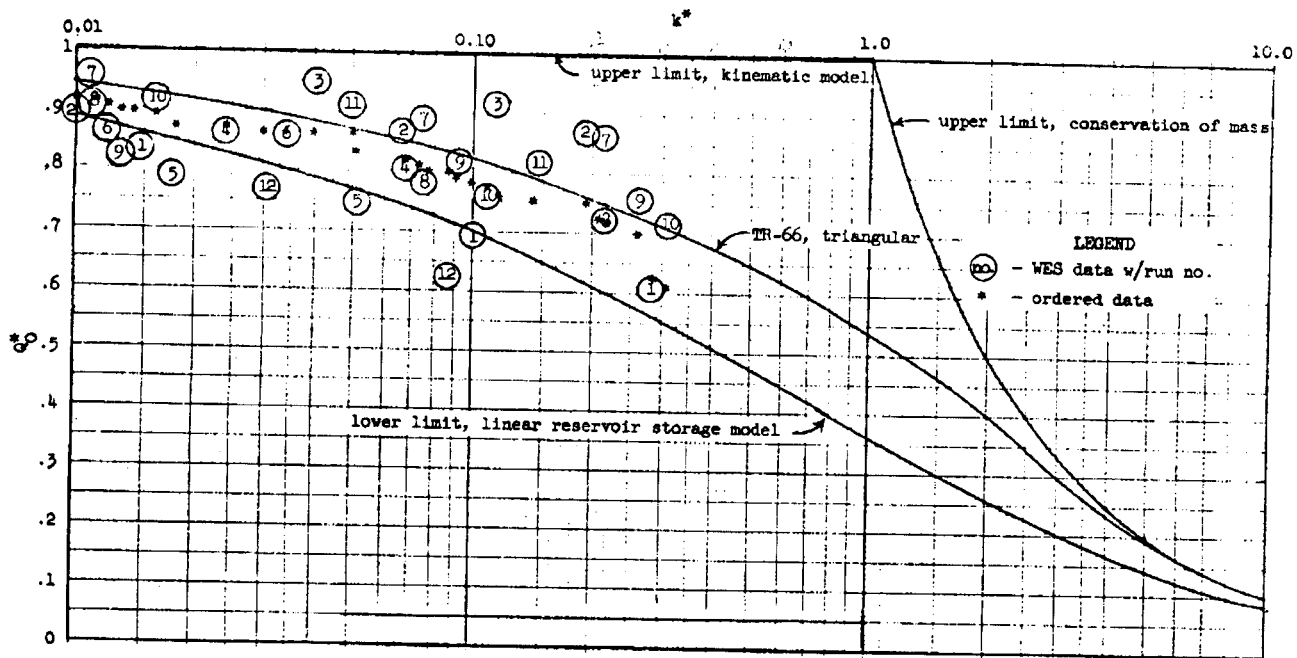


Figure 4. Smooth Channel Condition

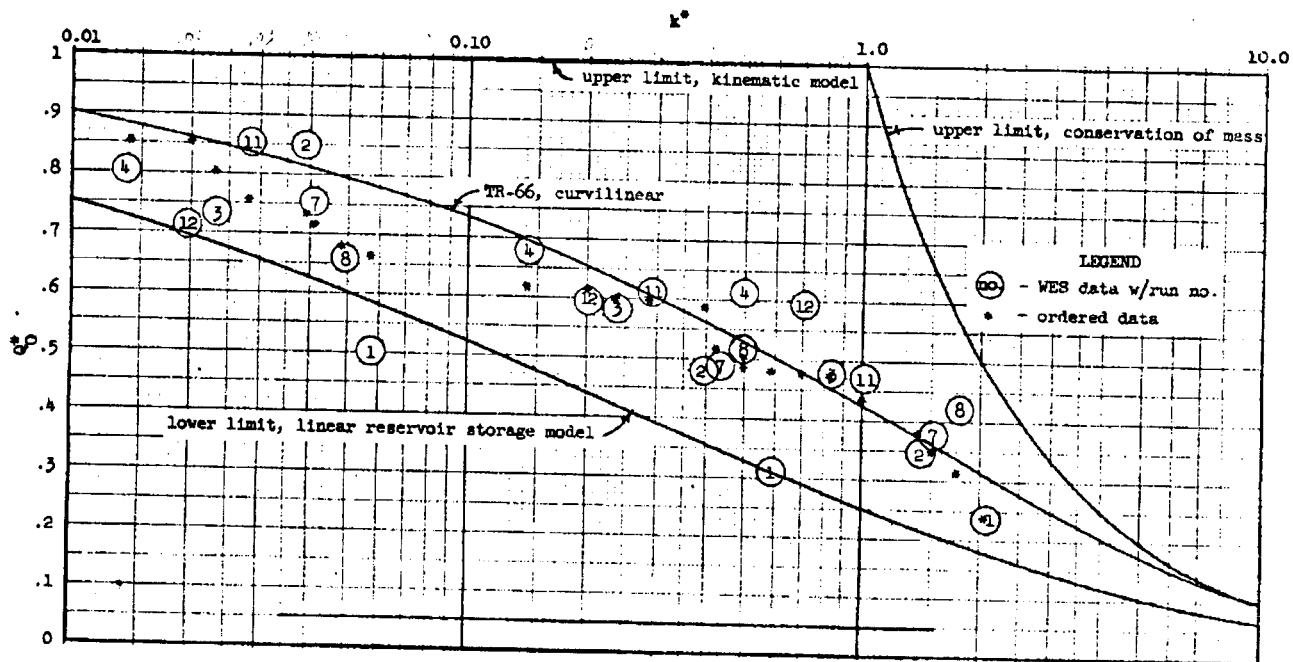


Figure 5. Rough Channel Condition

TABLE NO. 6
STATISTICAL DATA - BREACH-REACH ROUTING

Statistical Parameter	Channel Condition	Summary Results			
		Q_0^*	t_0^*	A_0^*	S_0^*
$\bar{\epsilon}$	Smooth	0.017	-0.084	-0.017	-0.005
$ \bar{\epsilon} $		0.055	0.084	0.065	0.010
S_d		0.079	0.074	0.077	0.017
S_e		0.082	0.113	0.080	0.018
r		0.741	0.942	0.369	0.993
r_m		0.561	0.728	0.239	0.930
$\bar{\epsilon}$		Rough	-0.003	0.023	0.014
$ \bar{\epsilon} $	0.052		0.073	0.065	0.030
S_d	0.078		0.104	0.089	0.052
S_e	0.079		0.108	0.092	0.053
r	0.948		0.987	0.706	0.984
r_m	0.921		0.881	0.657	0.914
$\bar{\epsilon}$	Combined		0.009	-0.041	-0.005
$ \bar{\epsilon} $		0.054	0.079	0.065	0.018
S_d		0.079	0.101	0.083	0.035
S_e		0.080	0.110	0.084	0.036
r		0.924	0.973	0.803	0.988
r_m		0.922	0.874	0.706	0.931

$$\epsilon_i = (\text{TR-66})_i - (\text{WES})_i$$

$$\bar{\epsilon} = \sum_i [\epsilon_i / N]$$

$$S_d = \sqrt{\left[\sum_i (\epsilon_i^2 / N) \right] - \bar{\epsilon}^2} \sqrt{\frac{N}{N-1}}$$

$$S_e = \sqrt{\sum_i (\epsilon_i^2 / N)} \sqrt{\frac{N}{N-2}}$$

always flush with the floor. Therefore, the statistical measures for the flow area do not include data at the breach itself ($L = 0$).

Table No. 6 shows that the discharge mean error for the combined conditions is less than 1% and the standard deviation is less than 8%. The discharge correlation coefficients were fair for the smooth condition and were excellent for the rough condition. These results are believed to be within the experimental error of the WES data.

The scatter of data caused by random error can be reduced by ordering the data by magnitude based on the plotted scatter diagram. If there is a functional relationship between the two variables, the ordered data give the most probable distribution of the relationship. The use and interpretation of order statistics are discussed in detail in the books by Mosteller and Rourke (5) and Mann et al (4).

The plotted data and the math model showed an inverse relationship between Q_0^* and k^* . The Q_0^* values were ordered in descending magnitude, beginning with the maximum to minimum. These order data were plotted versus the k^* values in ascending order of magnitude, beginning with the minimum to maximum. The plots of the ordered data in Figures 4 and 5 show that the TR-66 model is a correct functional form although it is generally conservative. The data also support the use of k^* as a correct non-dimensional basis for comparing routing results from varied hydrologic-hydraulic situations.

SUMMARY AND CONCLUSIONS

Scope of Applicability

TR-66 is applicable for studying the downstream flood potential from a dam-breach. This permits computation of data for a rational determination of dam classification, emergency flood preparedness studies, and flood plain zoning. For these purposes there is no need for accurate prediction of the actual breaching and establishment of downstream hydraulic conditions. Studies of this nature may be based on, if not limited to, the assumption of instantaneous breaches and initial downstream dry-bed conditions. This paper shows that TR-66 gives reasonable downstream predictions under the above assumptions when proper storage-discharge relationships are used.

Additional Study Needed

There is one important area that needs further study: the determination of the physical processes and subsequent math models of the actual breaching phenomena. This study will lead to more realistic predictions of the instantaneous peak discharge of the breach hydrograph.

Acknowledgements

The authors thank the engineers of the Design and Hydrology Units for their comments and suggestions in the development of this paper. Special thanks are due William H. Sammons for his help with the statistical analyses and interpretations of the data.

REFERENCES

1. Brevard, John A. and Theurer, Fred D. 1979. SIMPLIFIED DAM-BREACH ROUTING PROCEDURE, Technical Release No. 66. Soil Conservation Service.
2. Corps of Engineers. 1960. FLOODS RESULTING FROM SUDDENLY BREACHED DAMS, CONDITIONS OF MINIMUM RESISTANCE. Misc. Paper No. 2-374, Report 1. U. S. Army Engineer Waterways Experiment Station.
3. Corps of Engineers. 1961. FLOODS RESULTING FROM SUDDENLY BREACHED DAMS, CONDITIONS OF HIGH RESISTANCE. Misc. Paper No. 2-374, Report 2. U. S. Army Engineer Waterways Experiment Station.
4. Mann, Nancy R. et al. 1974. METHODS FOR STATISTICAL ANALYSIS OF RELIABILITY AND LIFE DATA. John Wiley and Sons, New York. 564 pp.
5. Mosteller, Frederick and Rourke, Robert E. K. 1973. STURDY STATISTICS. Chaps. 14 and 15. Addison-Wesley Publishing Co., Reading, Mass.
6. McCuen, Richard H. and Snyder, Willard M. 1975. A PROPOSED INDEX FOR COMPARING HYDROGRAPHS. Water Resources Research Vol. 11, No. 6.

